BULLETIN OF THE POLISH ACADEMY OF SCIENCES
TECHNICAL SCIENCES, Vol. 71(5), 2023, Article number: e147059
DOI: 10.24425/bpasts.2023.147059

Mechanical properties and Mullins effect in rubber reinforced by montmorillonite

Anita BIAŁKOWSKA[1]*, Małgorzata PRZYBYŁEK[1], Marta SOLA-WDOWSKA[1], Milan MASAŘ[2], and Mohamed BAKAR[1]

[1] University of Technology and Humanities in Radom, Faculty of Chemical Engineering and Commodity Science, Poland
[2] Tomaš Bata University in Zlin, Centre of Polymer Systems, Czech Republic

Abstract. The present work investigated the properties of rubber vulcanizates containing different nanoparticles (Cloisite 20A and Cloisite Na+) and prepared using different sonication amplitudes. The results showed that a maximum improvement in tensile strength of more than 60% over the reference sample was obtained by the nanocomposites containing 2 wt.% Cloisite 20A and 1 wt.% Cloisite Na+ and mixed with a maximum amplitude of 270 μm. The modulus at 300% elongation increased by approximately 18% and 25% with the addition of 2 wt.% Cloisite 20A and 3 wt.% Cloisite Na+, respectively. The shape retention coefficient of rubber samples was not significantly affected by the mixing amplitude, while the values of the softness measured at the highest amplitude (270 μm) were higher compared to those of mixtures homogenized with lower amplitudes. The loading-unloading and loading-reloading processes showed similar trends for all tested nanocomposites. However, they increased with increasing levels of sample stretching but were not significantly affected by filler content at a given elongation. More energy was dissipated during the loading-unloading process than during the loading-reloading. SEM micrographs of rubber samples before and after cycling loading showed rough, stratified, and elongated morphologies. XRD results showed that elastomeric chains were intercalated in the MMT nanosheets, confirming the improvement of mechanical properties. The difference between the hydrophilic pristine nanoclay (Cloisite Na+) and organomodified MMT (Cloisite 20A) was also highlighted, while the peaks of the stretched rubber samples were smaller, regardless of the rubber composition, due most probably to the decrease of interlayer spacing.

Key words: rubber nanocomposites; physical properties; Mullins effect; morphology.

1. INTRODUCTION

Due to their excellent elasticity, damping properties, shape retention, and weather resistance, elastomeric materials are used in various applications including the automotive industry, transport, building, thermal and electrical properties. However, their low stiffness makes them not always suitable for industrial applications. The addition of solid particles leads to improved material properties that make them more versatile for applications such as tires and machinery supports [1–3].

Due to outstanding properties, elastomer nanocomposites have attracted great interest in the last few decades [4–10]. The addition of a small amount of nanofillers significantly improves the mechanical, thermal, and flame retardancy of elastomers [4–6].

Nanocomposites were prepared by melting process [11–13], latex compounding [14, 15], and solution method [16, 17]. Lopez-Manchado *et al.* [11] prepared natural rubber (NR) nanocomposites containing modified bentonite by using the vulcanization method. The degree of crosslinking increased in the presence of the organoclay as confirmed by the accelerated vulcanization reaction results. However, polybutadiene rubber nanocomposites were prepared by Kim *et al.* [12] by using the melting mixing method. The obtained results showed that the tensile strength and the abrasion resistance of the nanocomposite were far superior to those of the unmodified rubber. Rebound resilience, compression set, and abrasion resistance were also increased. The improvement of the mechanical properties was attributed to intercalated rubber chains in the nanoclays interlayers.

Although relatively more complex, the latex mixing technique was used by Mitra *et al.* [15] to prepare nanocomposites based on natural rubber (NR) and styrene butadiene rubber (SBR) with unmodified montmorillonite clay (MMT Na^+). Results showed that the addition of 6 phr MMT improved the tensile strength and Young's modulus by 55% and 200%, respectively, in comparison with unfilled NR. Moreover, SBR-based nanocomposites exhibited improved mechanical properties and thermal stability.

Nanocomposites based on isobutylene-isoprene rubber were prepared by Liang *et al.* [17] using solution and melting methods. Mechanical and barrier properties were improved, due to the very good dispersion of nanoparticles. Moreover, the properties of the nanocomposites prepared by the solution method were superior to those obtained by the melt method.

As rubber nanocomposites are often used in applications where cyclic loadings are applied, research was conducted to investigate the stress softening during cyclic loading of filled rubbers, known as the Mullins effect [18–25]. A complete analysis of this phenomenon is very useful for the long-term safe

*e-mail: a.bialkowska@uthrad.pl

Manuscript submitted 2023-05-04, revised 2023-08-05, initially accepted for publication 2023-08-07, published in October 2023.

use of rubber materials. Due to the differences between the composites as well as the difficulties encountered in highlighting their microscopic structures, it remains very difficult to propose a unique interpretation of the Mullins effect. The interpretations that were advanced to explain the stress softening of filled rubbers include chain disentanglements which resulted in a decrease in the effective cross-link density [18–22], chain breakage at the interface between the rubber and the fillers [23–26], sliding of the short rubber chains [20, 27–29], and destruction of the filler aggregates [18, 30, 31]. However, Marckmann *et al.* [32] stipulated that the rupture of chain-filler and chain-chain bonds occurs during the stretching of rubber samples.

The purpose of the present study was to investigate the effect of montmorillonites on the mechanical properties and Mullins effect of rubber nanocomposites. It is expected that the cycling loading will be attenuated by the presence of nanoclays in the rubber materials.

2. EXPERIMENTAL

2.1. Materials

The following main raw materials were used to prepare rubber nanocomposites. The proportions are given in Table 1.

- KER®N-29 Rubber – acrylonitrile-butadiene rubber, obtained from Synthos Rubbers, Oświęcim, Poland;
- SVR-3L Natural Rubber – from Dau Tieng Rubber Corporation, Vietnam;
- Zinc oxide – (Huta Będzin, Będzin, Poland);
- Glyceryl tristearate – (Poch S.A, Gliwice);
- Cloisite 20A – montmorillonite modified with quaternary ammonium salts (dimethyl dihydrogenated tallow ammonium cations);
- Cloisite Na^+ – natural unmodified montmorillonite;
- Santicizer 261A – (phthalate alkyl (C7–C9) benzyl) – plasticizer from Brenntag Co. Kędzierzyn Koźle, Poland;
- Accelerator T – used as an accelerator during vulcanization of rubber from Rubber Industry, Miekinia, Blonie, Poland;
- Accelerator DM – dibenzothiazole disulfide from Radka Company, Miękinia – Błonie, Poland;
- Sulphur – produced by Siarkopol, Tarnobrzeg, Poland.

Table 1
Composition of rubber mixtures based on KER N-29 and SVR-3L rubbers and other ingredients (The weight in the mixture is expressed in kgs)

MMT content (wt.%)	0	1	2	3
KER N-29 Rubber	1.200			
SVR-3L Rubber Zinc oxide	0.200 0.150			
Glyceryl tristearate / Stearin	0.030			
Dispersion Cloisite (20A or Na+) + Santacizer 261A	–	0.012 + 0.040	0.024 + 0.080	0.036 + 0.120
Santicizer 261A	0.200	0.160	0.120	0.080
Brown factice	0.300			
Chalk	0.800			
Wax	0.030			
Aflux	0.010			
Accelerator T	0.008			
Accelerator DM	0.020			
Sulphur	0.008			
Total weight	2.956	2.968	2.980	2.992

2.2. Preparation of elastomer nanocomposites

A series of rubber mixtures were prepared with different amounts (1 wt.%, 2 wt.%, and 3 wt.%) of montmorillonite (Cloisite 20A and Cloisite Na+). First, montmorillonite (MMT) dispersions were prepared with the plasticizer Santicizer 261A, which were then mechanically mixed for 10 minutes at room temperature followed by ultrasonic homogenization with a Hielscher model UP200H (under different amplitudes: 162 μm, 216 μm, and 270 μm) for 15 minutes. The plasticization of the mixtures was carried out in two industrial roller mills at 50–60°C for 10 minutes. The other ingredients were then incorporated and mixed together. The vulcanization process was carried out for 15 minutes using a press at temperatures between 150 and 160°C and a pressure of 10 MPa (Fig. 1).

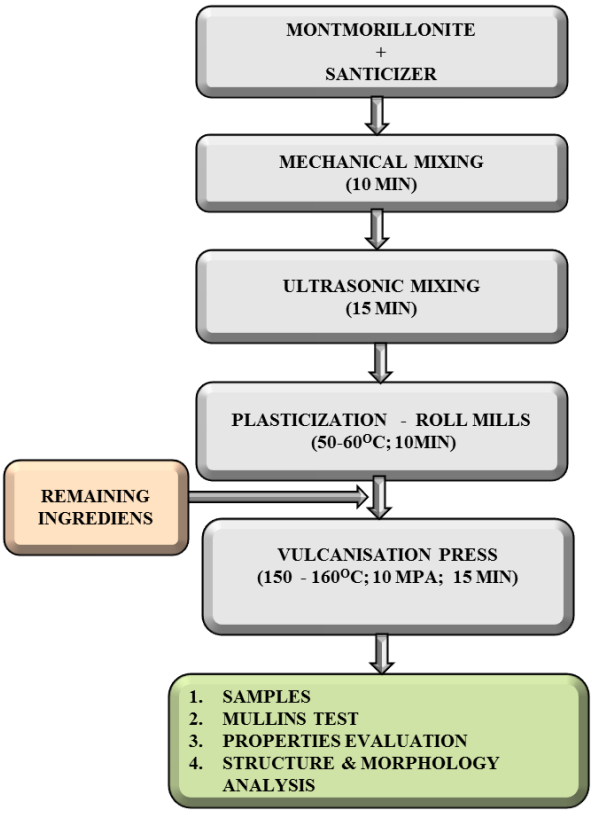

Fig. 1. Steps for the preparation and evaluation of properties of rubber nanocomposites

The vulcanizates were left to cool in the moulds, then the samples of defined shapes and sizes were cut out for further testing.

2.3. Evaluation of rubber sample properties

The tensile strength and strain at break were evaluated on dumbbell-shaped specimens according to PN-ISO 37:2007 and a deformation rate of 200 mm/min with an Instron machine.

The Shore A hardness test of the elastomer samples was carried out at room temperature on disks 10 mm thick and 100 mm in diameter in accordance with PN-80/C-04238.

The softness of the samples was determined at room temperature by using the Shopper method according to PN-54/C-04249 Rubber. The measurement employed a metallic ball with a diameter of 10 mm and a load of 10.3 N. The softness of the vulcanizates was calculated from the formula:

$$H = \frac{10.3}{\pi \times h \times D}, \tag{1}$$

where: H – softness, (N/m^2); h – the defection of the sample, (m); D – ball diameter (= 0.01 m).

The shape retention coefficient also known as the elastic recovery was determined based on measurements of the sample deformation after compression at room temperature, in accordance with the PN-ISO 815:1998 standard. The tests were carried out using the Zwick/Roell Z010 testing machine on cylindrical samples with a diameter of 32 mm. The shape retention coefficient (K_S) was calculated using the following equation:

$$K_s = \frac{h_2 - h_1}{h_0 - h_1}, \tag{2}$$

where: K_S – shape retention coefficient, (−); h_0 – sample height before the test, (mm); h_1 – sample height when compressed by 20% of its height, (mm); h_2 – sample height 5 minutes after the end of the measurement, (mm).

The Mullins effect was evaluated on rubber specimens which were subjected to a sequence of cyclic tensile tests with increasing maximum pre-strains of 100% at each cycle. The test was performed using a universal Instron machine at room temperature and a crosshead head speed of 50 mm. min^{-1}.

2.4. Structure and morphology characterization

The morphology of the rubber samples was analyzed with a NovaNano SEM 450 microscope (The Netherlands, FEI company). The elemental microanalysis was performed by the Octane SSD (area 30 mm2) EDX (energy-dispersive X-ray) detector (AMETEC, Inc.). Images were taken using an ETD (topographic contrast) and CBS (material contrast) detector at accelerating 5 kV and 15 kV voltages, respectively.

X-ray diffraction (XRD) tests of nanocomposite samples were performed using a diffractometer MiniFlex600 (Japan, RIGAKU) with Co cathode and a scanning speed of 6?/min. The voltage and emission current were set at 40 kV and 30 mA, respectively. The wavelength of used radiation is $\lambda(\mathrm{CoK}\alpha 1,2) = 0.179$ nm.

3. RESULTS AND DISCUSSION

Figure 2 shows the tensile strength (TS) of rubber composites containing different amounts of montmorillonite (MMT) and mixed with a maximum sonication amplitude of 270 μm. It was shown that TS increased then decreased with increasing MMT content, and the maximum improvement in TS of approximately 65% and 60% over the reference sample was achieved with 2 wt.% Cloisite 20A and 1 wt.% Cloisite Na+, respectively. However, an increase of about 10% (which is within the experimental error range) was obtained with 1 wt.% of Cloisite Na+. The improvement in tensile strength can be attributed to the intercalation/exfoliation processes of nanoparticles in the rubber nanocomposites as confirmed elsewhere [15, 33]. The occurrence of such processes generally results in increased interlayer spacing and, consequently the enhancement of the nanocomposite performance properties.

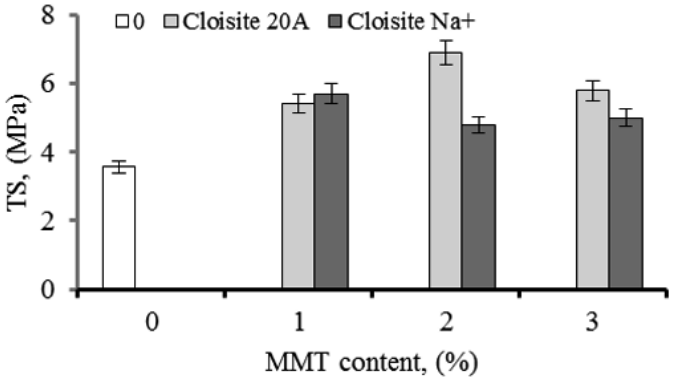

Fig. 2. The effect of montmorillonite (Cloisite 20A and Cloisite Na+) content on the stress at break of rubber samples prepared with a mixing amplitude of 270 μm

The effect of montmorillonite type and content (Cloisite 20A and Cloisite Na+) on the tensile strength (TS) of rubber composites homogenized with amplitudes of 216 μm and 162 μm is shown in Figs. 3 and 4, respectively. From the results of Fig. 3, it can be seen that an increase of approximately 55% and 35% (compared to the rubber sample without nanoparticles) was obtained with the rubber nanocomposites containing 2 wt.% Cloisite Na+ and 1 wt.% Cloisite 20A, respectively.

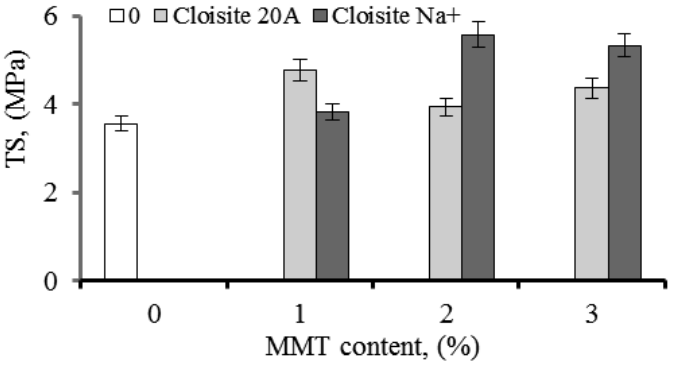

Fig. 3. The effect of montmorillonite (MMT – Cloisite 20A and Cloisite Na+) content on the tensile strength (TS) of rubber samples prepared with mixing amplitudes of 216 μm

However, in the case of the lowest mixing amplitude (Fig. 4), the only increase in TS was exhibited by the rubber nanocomposites based on Cloisite Na+ with a maximum reaching 30% at 3 wt.% of nanoclay. In addition, it should be noted that the strength of the rubber samples containing Cloisite Na+ was no higher than that of the Cloisite 20A-based samples. Also, as expected, the lowest sonication amplitude associated with lower energy delivered to the systems does not lead to better mixing and thus improved properties. The improvement in tensile strength of rubber nanocomposites can be caused by the exfoliation and/or intercalation of the nanoparticles, as is the case with other polymer nanocomposites [6, 17, 34]. On the other hand, the decrease in properties is generally explained by the agglomeration of the nanoparticles.

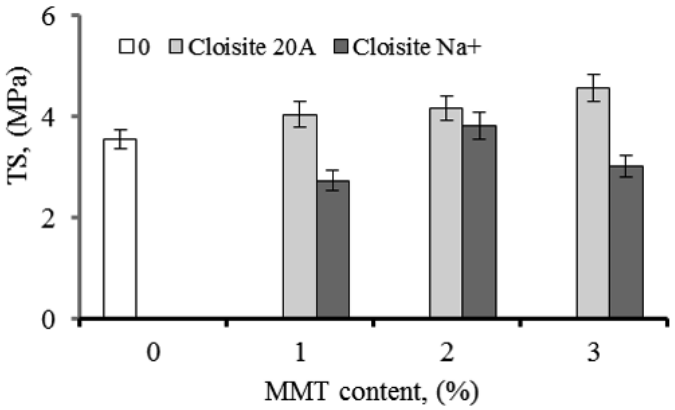

Fig. 4. The effect of montmorillonite (MMT – Cloisite 20A and Cloisite Na+) content on the tensile strength (TS) of rubber samples prepared with mixing amplitudes of 162 μm

It is well known that ultrasonic processing leads to increased efficiency in mixing and nanoparticle dispersion. In addition, a higher sonication amplitude provides more energy to the system, which facilitates an efficient disaggregation of the clay layers, and thus the formation of exfoliated nanocomposites with improved properties.

The strain at break of rubber samples prepared with a mixing amplitude of 270 μm is shown in Fig. 5 as a function of montmorillonite content. A slight increase in strain at break was exhibited only by nanocomposites containing 1 wt.% of Cloisite Na+ or 2 wt.% of Cloisite 20A, most probably due to strong bonding between the nanoparticles and the rubber chains.

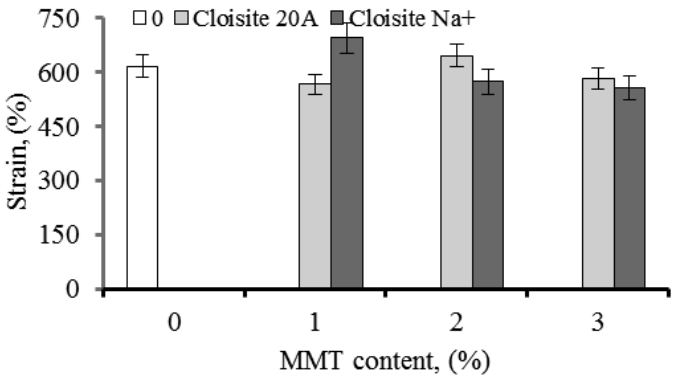

Fig. 5. The effect of montmorillonite (Cloisite 20A and Cloisite Na+) content on the tensile strain at break of rubber samples prepared with mixing amplitudes of 270 μm

Table 2 shows the effect of montmorillonite content on the stiffness of rubber vulcanizates as expressed by the modulus at 300% elongation. It can be observed that the modulus values of the samples homogenized with mixing amplitudes of 162 μm or 216 μm were lower by 20% than that obtained with the highest amplitude (i.e. 270 μm). Moreover, the modulus measured at a mixing amplitude of 270 μm increased with increasing amount of added MMT Cloisite 20A. A maximum increase in modulus of about 18% and 25% was obtained with the addition of 2 wt.% of Cloisite 20A and 3 wt.% of Cloisite Na+, respectively.

Table 2

The effect of montmorillonite (Cloisite 20A and Cloisite Na^+) content and mixing amplitudes on the values of modulus at 300% elongation

Cloisite 20A			Cloisite Na^+		
Mixing amplitude, (μm)	MMT content, (%)	Modulus at 300%, (MPa)	Mixing amplitude (μm)	MMT content (%)	Modulus at 300%, (MPa)
–	0	1.83	–	0	1.83
270	1	2.59	270	1	2.17
	2	2.71		2	2.32
	3	2.68		3	2.85
216	1	2.29	216	1	1.74
	2	2.20		2	2.00
	3	1.89		3	1.95
162	1	2.44	162	1	2.97
	2	2.41		2	2.01
	3	2.57		3	2.06

However, rubber nanocomposites containing 3 wt.% Cloisite Na^+ showed an increase of about 25% in modulus compared to the reference sample. At the lowest mixing amplitude (i.e. 162 μm corresponding to 60% of the maximum amplitude), the highest value of the modulus was exhibited by rubber nanocomposite based on 1 wt.% of Cloisite Na^+.

The values of the coefficient of shape retention and softness of vulcanizates are shown in Table 3 as a function of montmorillonite content and ultrasonic amplitude of mixing. Crosslinked rubber generally offers good shape retention properties. The rubber samples contained 1, 2, and 3 wt.% of Cloisite 20A or Cloisite Na+ and were mixed with different sonication amplitudes (270, 216, and 162 μm). It can be noted that the coefficient of shape retention of rubber samples was not significantly affected by the highest mixing amplitude (270 μm) and the intermediate one (i.e. 216 μm which is equivalent to 80% of the maximum amplitude), regardless of the amount of added montmorillonite (MMT).

However, the softness values of the nanocomposite samples mixed with an amplitude of 162 μm were significantly lower than those homogenized at amplitudes of 216 μm or 270 μm.

Table 3

The shape retention coefficient of the tested compositions and softness of vulcanizates as the function of the amount and type of montmorillonite (Cloisite 20A, Cloisite Na^+) and the amplitude of mixing

	MMT content, (%)	Coefficient of shape retention Ks, (–)			Softness, (MN/m^2)		
		Amplitude of mixing, (μm)					
		270	216	162	270	216	162
	0	0.99	0.99	0.99	0.57	0.57	0.57
Cloisite 20A	1	0.94	0.93	0.80	0.56	0.58	0.29
	2	0.96	0.98	0.91	0.57	0.58	0.28
	3	0.98	0.98	0.94	0.58	0.61	0.28
Cloisite Na^+	1	0.98	0.96	0.93	0.56	0.40	0.24
	2	0.98	0.95	0.94	0.57	0.39	0.26
	3	0.96	0.98	0.93	0.56	0.38	0.27

The decrease in the softness for all rubber nanocomposites was between 48% and 58%, compared to the reference sample. The highest sonication amplitude (i.e. 270 μm) which induced the best tensile strength and modulus at 300% elongation of rubber samples was selected for Mullins effect tests.

The hardness of virgin rubber vulcanizate (43 Shore A) increased by approximately 10% with Cloisite 20A and remained unchanged with the addition of Cloisite Na+.

As schematically shown in Fig. 6, the Mullins effect consists of loading-unloading tests of rubber samples each time at a higher level of elongation after each cycle. The unstretching of the sample occurs at lower loads and the load required to re-stretch the sample is lower than during the previous load. It can be observed that changes occur in the mechanical response of the sample after being loaded, unloaded, and reloaded. The sample becomes softer after each loading-unloading cycle probably due to the breaking of the bonds between the rubber and the nanofillers. Various studies confirmed that the Mullins effect existed in both the virgin rubber as well as filled rubber system [20, 25]. Although the Mullins effect has been studied for several decades, there are still unclear aspects of this phenomenon and the properties of rubber nanocomposites.

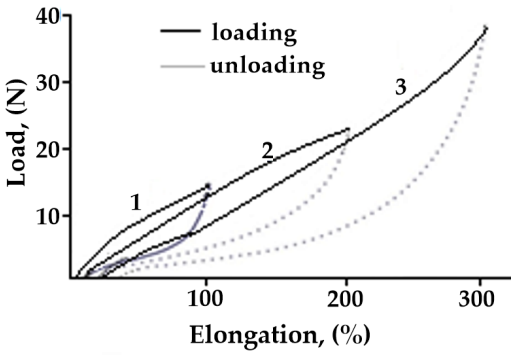

Fig. 6. The presentation of loading-unloading reloading cycles of a rubber sample containing 1 wt.% of Cloisite Na+ and showing Mullins effect

Figure 7 shows a schematic presentation of the loading-unloading cycles of a rubber sample showing the Mullins effect. The difference between the stored elastic energy during the sample loading and its release elastic energy during its unloading is related to deformation of the system. The sample exhibits a residual strain or permanent set after unloading.

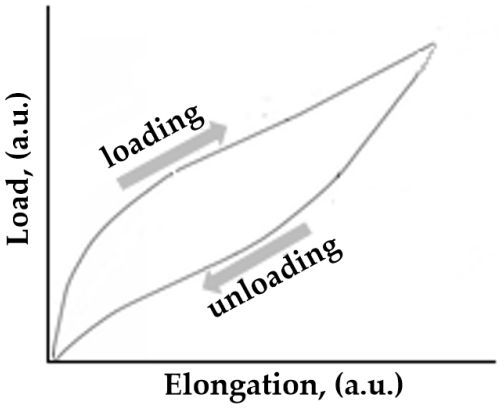

Fig. 7. Schematic presentation of loading-unloading cycles of a rubber sample showing Mullins effect

However, Fig. 8 illustrates a schematic presentation of the difference between the stored elastic energy during the loading and reloading processes. It was reported that the energy during the loading followed by reloading depends on the structure of the rubber, mainly its degree of crosslinking as well as the characteristics of the nanofillers [25, 30]. According to Li *et al.* [35], the softening of rubber samples depends on several factors such as test temperature, type and content of filler, crosslinking agent, and loading and unloading speed. The unloading curve was always below the reloading one, due to the damage to the rubber structure during the loading process.

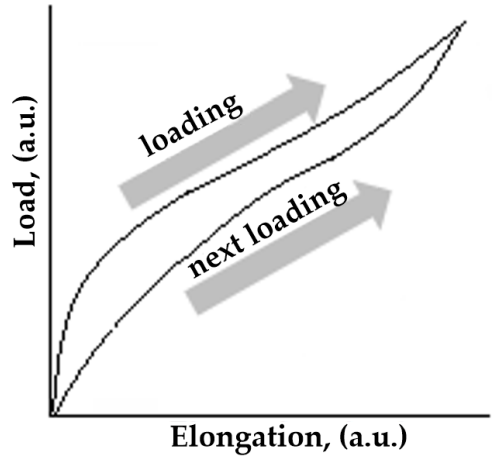

Fig. 8. The difference between the stored elastic energy during loading-reloading processes

Table 4 contains the difference between the stored elastic energy during loading and released energy during unloading of the rubber samples at maximum mixing sonication amplitude

(i.e. 270 μm). The energy losses associated with each recovery hysteresis at a fixed crosshead speed are analyzed as a function of sample elongation. It can be observed that the energy loss for each composite increased with the increase in the level of sample stretching. However, it was not significantly affected by increasing filler content at a given elongation. The recovery hysteresis involves small deformations of the rubber phase in the nanocomposites as reported elsewhere and/or breakage of bonds between the rubber phase and nanoparticles. However, it has been shown that the softening of samples stretched at room temperatures can be recovered at higher temperatures or after a longer standing time.

Table 4
Energy (J) between the loading and subsequent unloading (at amplitude 270 μm)

	MMT content, (%)	Elongation, (%)						
		100	200	300	400	500	600	700
–	0	0.09	0.28	0.43	0.65	0.97	1.30	–
Cloisite 20A	1	0.09	0.29	0.49	–	–	–	–
	2	0.11	0.31	0.51	0.80	1.17	–	–
	3	0.11	0.35	0.59	0.90	1.27	–	–
Cloisite Na^+	1	0.12	0.30	0.46	0.67	0.97	1.29	1.69
	2	0.11	0.31	0.47	0.75	1.03	1.73	–
	3	0.09	0.27	0.45	0.66	0.96	–	–

The difference between the stored elastic energies for loading-reloading cycles at a sonication amplitude of 270 μm is shown in Table 5. Similarly to the results in Table 4, the energy values increased with the growing level of sample stretching, while they were not affected by the amount of added nanoparticles. It is seen that the energy is lower than that of recovery hysteresis (Table 4). Moreover, the energy involved in the loading-unloading is higher than that of the loading-reloading process, due to the damage of the rubber structure.

Table 5
Energy (J) between the loading and the reloading processes (at amplitude 270 μm)

	MMT content, (%)	Elongation, (%)						
		100	200	300	400	500	600	700
	0	0.07	0.17	0.22	0.35	0.53	0.74	–
Cloisite 20A	1	0.06	0.19	0.27	–	–	–	–
	2	0.08	0.19	0.28	0.44	0.67	–	–
	3	0.07	0.19	0.33	0.47	0.70	–	–
Cloisite Na^+	1	0.06	0.17	0.25	0.37	0.53	0.69	0.93
	2	0.07	0.19	0.27	0.37	0.88	0.98	–
	3	0.06	0.18	0.26	0.39	0.55	–	–

It was confirmed that the rubber matrix and the interfacial region show different softening behaviors and that the recovery of the nanocomposite comes mainly from the recovery of the interfacial region because the rubber matrix takes longer to recover [24].

Figure 9 shows the micrographs of rubber samples before and after cycling loading. The fracture surface of rubber vulcanizate without nanofiller (designated by "0") is rough and more stratified. However, as expected the samples exhibited elongated and rough morphologies after stretching. The roughness of fractured surfaces was induced by added solid nanoparticles which showed strong interfacial adhesion with the rubber phase, as reported elsewhere [36]. The lack of changes in the morphology can be due to the recovery of samples with time as reported in the literature [37–40].

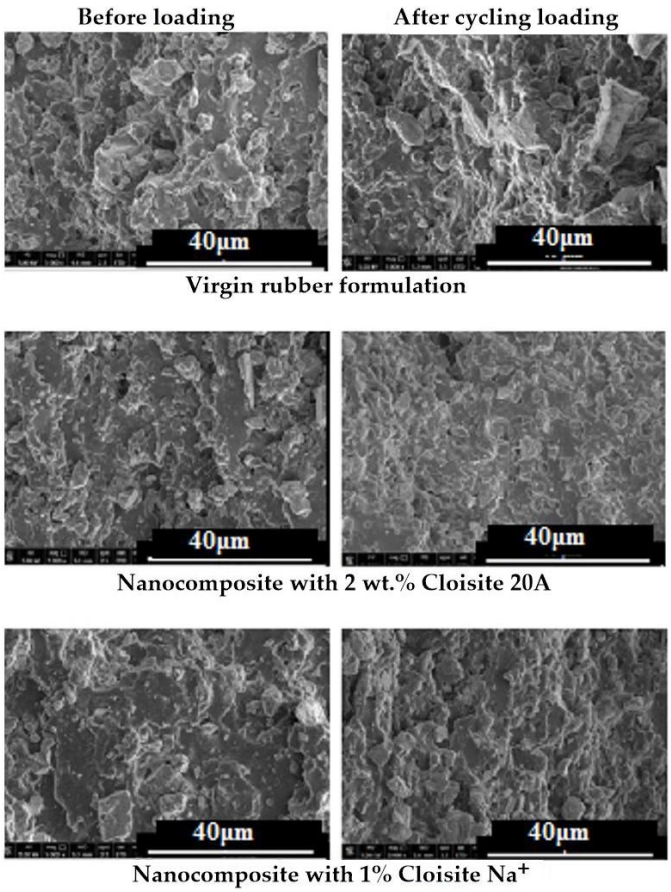

Fig. 9. Micrographs of rubber samples before and after cycling loading

Figure 10 shows XRD diagram of rubber samples before and after cycling stretching. Rubber samples before stretching without nanoclays, those containing 2 wt.% Cloisite 20A and 1 wt.% Cloisite Na+ are denoted "O", "20A" and "Na" respectively.

The stretched samples are denoted respectively by "HO", "H20A" and "HNa". The X-ray diffraction (XRD) patterns of

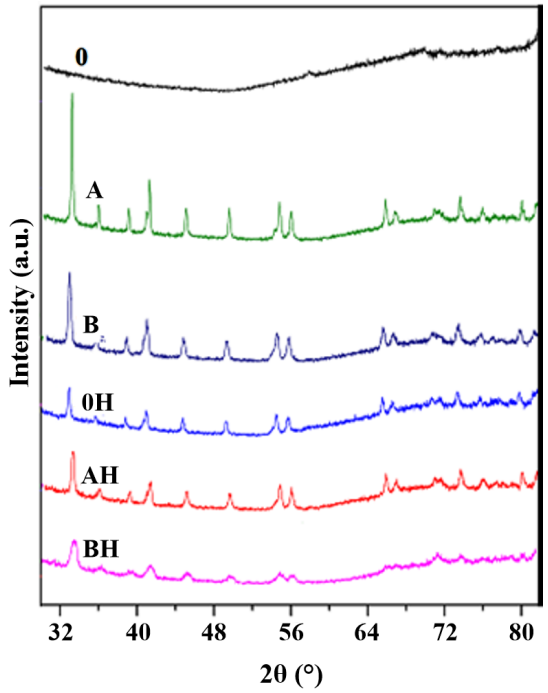

Fig. 10. XRD of rubber nanocomposite samples

rubber samples before and after cycling stretching are shown in Fig. 9. Rubber samples before stretching without nanoclays, and those containing 2 wt.% Cloisite 20A and 1 wt.% Cloisite Na+ are denoted "O", "20A" and "Na", respectively. The stretched samples are denoted by "HO", "H20A" and "HNa", respectively. The results confirmed that elastomeric chains are embedded in the MMT nanosheets, leading to the intercalation process, responsible for the improvement of mechanical properties. The difference between the hydrophilic pristine nanoclay (Cloisite Na+) and organomodified MMT (Cloisite 20A) is also highlighted. Moreover, the peaks of stretched rubber samples are smaller, regardless of the rubber composition, due most probably to the decrease of interlayer spacing as represented in Fig. 11.

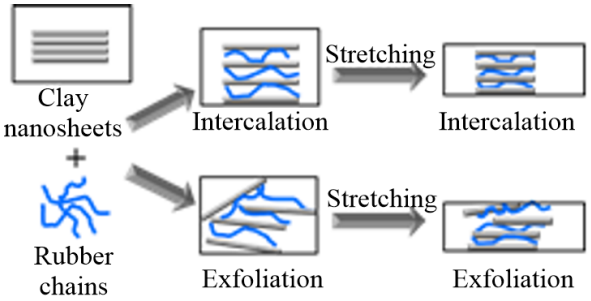

Fig. 11. Stretching of intercalated and exfoliated nanocomposite samples

The stretching of the sample conducts to the straightening of rubber chains and nanoplatelets and thus to the decrease of interlayer distance.

4. CONCLUSIONS

From the obtained results it can be stated that:

The nanocomposites containing 2 wt.% Cloisite 20A and 1 wt.% Cloisite Na+, and blended with a maximum amplitude of 270 μm showed a maximum improvement in tensile strength of more than 60% compared to the sample of reference. The modulus at 300% elongation increased by approximately 18% and 25% with the addition of 2 wt.% of Cloisite 20A and 3 wt.% of Cloisite Na+, respectively.

The mixing amplitude did not affect the shape retention of rubber samples, while the values of the softness measured at the highest amplitude (270 μm) were higher compared to those of mixtures homogenized with lower amplitudes. The hardness of the rubber samples did not change significantly with the addition of Cloisite Na+ or Cloisite 20A.

Results from Mullins tests indicated that the energy loss during the loading-unloading or loading-reloading processes had similar trends for all nanocomposites. They increased with increasing levels of sample stretching, while they were not significantly affected by filler content increase at a given elongation. More energy was dissipated during the loading-unloading process than during the second process.

SEM micrographs of rubber samples before and after cycling loading showed rough, stratified, and elongated surfaces. XRD results showed that rubber chains are embedded in the MMT nanosheets, confirming the occurrence of the intercalation process, responsible for the improvement of mechanical properties. The difference between the hydrophilic pristine nanoclay (Cloisite Na+) and organomodified montmorillonite (Cloisite 20A) was also confirmed. The peaks of stretched rubber samples were smaller, regardless of the rubber composition, due to the decrease in interlayer spacing.

REFERENCES

[1] L. Bokobza, "The Reinforcement of Elastomeric Networks by Fillers," *Macromol. Mater. Eng.*, vol. 289, no. 7, pp. 607–621, 2004, doi: 10.1002/mame.200400034.

[2] L. Tadiello, S. Guerra, and L. Giannini, "Sepiolite-Based Anisotropic Nanoparticles: A New Player in the Rubber Reinforcement Technology for Tire Application," *Appl. Sci.*, vol. 12, no. 5, 2022, doi: 10.3390/app12052714.

[3] G. Heinrich, M. Klüppel, and T.A. Vilgis, "Reinforcement of elastomers," *Curr. Opin. Solid State Mater. Sci.*, vol. 6, no. 3, pp. 195– 203, 2002, doi: 10.1016/S1359-0286(02)00030-X.

[4] L. Gu, H. Nan, R. Xing, G. Pan, Y. Wang, and X. Ge, "Mechanical and thermal performances of styrene butadiene rubber nanocomposites with boron nitride nanosheets, carbon nanotubes, and the hybrid filler system," *Polym Compos.*, vol. 44, no. 1, pp. 480–491, 2023, doi: 10.1002/pc.27111.

[5] A.S. Sethulekshmi, A. Saritha, and K. Joseph, "A comprehensive review on the recent advancements in natural rubber nanocomposites," *Int. J. Biol. Macromol.*, vol. 194, pp. 819–842, 2022, doi: 10.1016/j.ijbiomac.2021.11.134.

[6] S.K. Srivastava and Y.K. Mishra, "Nanocarbon reinforced rubber nanocomposites: detailed insights about mechanical, dynamical mechanical properties, payne, and mullin effects," *Nanomaterials*, vol. 8, no. 11, 2018, doi: 10.3390/nano8110945.

[7] D.Z. Pirityi, T. Barany, and K. Pölöskei, "Hybrid reinforcement of styrene-butadiene rubber nanocomposites with carbon black, silica, and grapheme," *J. Appl. Polym. Sci.*, vol. 139 no. 32, p. e52766, 2022, doi: 10.1002/app.52766.

[8] X. Li, J. Liu, and Z.J. Zheng, "Recent progress of elastomer–silica nanocomposites toward green tires: simulation and experiment," *Polym. Int.*, vol. 72, vo. 9, pp. 764–782, 2023, doi: 10.1002/pi.6454.

[9] A. Alipour, G. Naderi, G.R. Bakhshandeh, H. Vali, and S. Shokoohi, "Elastomer nanocomposites based on NR/EPDM/organoclay: morphology and properties," *Int. Polym. Process.*, vol. 26, no. 1, pp. 48–55, 2011, doi: 10.3139/217.2381.

[10] S.M. Liff, N. Kumar, and G.H. McKinley, "High-performance elastomeric nanocomposites via solvent-exchange processing," *Nat. Mater.*, vol. 6, no. 1, pp. 76–83, 2007, doi: 10.1038/nmat1798.

[11] M.A. Lopez-Manchado, B. Herrero and M.J.P.I. Arroyo, "Preparation and characterization of organoclay nanocomposites based on natural rubber," *Polym. Int*., vol. 52, no. 7, pp. 1070–1077, 2003, doi: 10.1002/pi.1161.

[12] M.S. Kim, D.W. Kim, S. Ray Chowdhury and G.H. Kim, "Melt-compounded butadiene rubber nanocomposites with improved mechanical properties and abrasion resistance," *J. Appl. Polym. Sci.*, vol. 102, no. 3, pp. 2062–2066, 2006, doi: 10.1002/app.23738.

[13] M. Zarei, G. Naderi, G.R. Bakhshandeh, and S. Shokoohi, "Ternary elastomer nanocomposites based on NR/BR/SBR: effect of nanoclay composition," *J. Appl. Polym. Sci.*, vol. 127, no. 3, pp. 2038–2045, 2013, doi: 10.1002/app.37687.

[14] L. Zhang, Y. Wang, Y. Wang, Y. Sui, and D. Yu, "Morphology and mechanical properties of clay/styrene-butadiene rubber nanocomposites," *J. Appl. Polym. Sci.*, vol. 78, no. 11, pp. 1873–1878, 2000, doi: 10.1002/1097-4628(20001209)78:11<1873::AID-APP40>3.0.CO;2-8.

[15] S. Mitra, S. Chattopadhyay, and A.K. Bhowmick, "Preparation and characterization of elastomer-based nanocomposite gels using an unique latex blending technique," *J. Appl. Polym. Sci.*, vol. 118, no. 1, pp. 81–90, 2010, doi: 10.1002/app.32389.

[16] M. Ganter, W. Gronski, P. Reichert, and R. Mülhaupt, "Rubber nanocomposites: morphology and mechanical properties of BR and SBR vulcanizates reinforced by organophilic layered silicates," *Rubber Chem. Technol.*, vol. 74, no. 2, pp. 221–235, 2001, doi: 10.5254/1.3544946.

[17] Y. Liang, Y. Wang, Y. Wu, Y. Lu, H. Zhang, and L. Zhang, "Preparation and properties of isobutylene–isoprene rubber (IIR)/clay nanocomposites," *Polym. Test.*, vol. 24, no. 1, pp. 12–17, 2005, doi: 10.1016/j.polymertesting.2004.08.004.

[18] A. Maiti *et al.*, "Mullins effect in a filled elastomer under uniaxial tension," *Phys. Rev. E*, vol. 89, no. 1, p. 012602, 2014, doi: 10.1103/PhysRevE.89.012602.

[19] C. Ma, T. Ji, C.G. Robertson, R. Rajeshbabu, J. Zhu, and Y. Dong, "Molecular insight into the Mullins effect: irreversible disentanglement of polymer chains revealed by molecular dynamics simulations," *Phys. Chem. Chem. Phys.*, vol. 19, no. 29, pp. 19468–19477, 2017, doi: 10.1039/C7CP01142C.

[20] W. Fu *et al.*, "Mechanical properties and Mullins effect in natural rubber reinforced by grafted carbon black," *Adv. Polym. Technol.*, vol. 2019, p. 4523696, 2019, doi: 10.1155/2019/4523696.

[21] Y. Song, R. Yang, M. Du, X. Shi, and Q. Zheng, "Rigid nanoparticles promote the softening of rubber phase in filled vulcanizates," *Polymer*, vol. 177, pp. 131–138, 2019, doi: 10.1016/j.polymer.2019.06.003.

[22] J.M. Clough, C. Creton, S.L. Craig, and R.P. Sijbesma, "Covalent bond scission in the Mullins effect of a filled elastomer: real-time visualization with mechanoluminescence," *Adv. Funct. Mater.*, vol. 26, no. 48, pp. 9063–9074, 2016, doi: 10.1002/adfm.201602490.

[23] H. Khajehsaeid, "Development of a network alteration theory for the Mullins-softening of filled elastomers based on the morphology of filler–chain interactions," *Int. J. Solids Struct.*, vol. 80, pp. 158–167, 2016, doi: 10.1016/j.ijsolstr.2015.10.032.

[24] X. Liang and K. Nakajima, "Study of the Mullins effect in carbon black- filled styrene–butadiene rubber by atomic force microscopy nanomechanics," *Macromolecules*, vol. 55, no. 14, pp. 6023–6030, 2022, doi: 10.1021/acs.macromol.2c00776.

[25] M. Qian *et al.*, "The influence of filler size and crosslinking degree of polymers on Mullins effect in filled NR/BR composites," *Polymers*, vol. 13, no. 14, p. 2284, 2021, doi: 10.3390/polym13142284.

[26] Y. Pan and Z. Zhong, "Modeling the Mullins effect of rubber-like materials," *Int. J. Damage Mech.*, vol. 26, no. 6, pp. 933–948, 2017, doi: 10.1177/1056789516635728.

[27] S. Cantournet, R, Desmorat, and J. Besson, "Mullins effect and cyclic stress softening of filled elastomers by internal sliding and friction thermodynamics model," *Int. J. Solids Struct.*, vol. 46, no. 11–12, pp. 2255–2264, 2009, doi: 10.1016/j.ijsolstr.2008.12.025.

[28] H. Wan *et al.*, "Chemical bond scission and physical slippage in the Mullins effect and fatigue behavior of elastomers," *Macromolecules*, vol. 52, no. 11, pp. 4209–4221, 2019, doi: 10.1021/acs.macromol.9b00128.

[29] P. Zhu and Z. Zhong, "Constitutive modelling for the mullins effect with permanent set and induced anisotropy in particle-filled rubbers," *Appl. Math. Model.*, vol. 97, pp. 19–35, 2021, doi:10.1016/j.apm.2021.03.031.

[30] J. Diani, B. Fayolle, and P. Gilormini, "A review on the Mullins effect," *Eur. Polym. J.*, vol. 45, no. 3, pp. 601–612, 2009, doi: 10.1016/j.eurpolymj.2008.11.017.

[31] S. Krpovic, K. Dam-Johansen, and A.L. Skov, "Importance of Mullins effect in commercial silicone elastomer formulations for soft robotics," *J. Appl. Polym. Sci.*, vol. 138, no. 19, p. 50380, 2021, doi: 10.1002/app.50380.

[32] G. Marckmann, E. Verron, L. Gornet, G. Chagnon, P. Charrier, and P. Fort, "A theory of network alteration for the Mullins effect," *J. Mech. Phys. Solids*, vol. 50, no. 9, pp. 2011–2028, 2002, doi: 10.1016/S0022-5096(01)00136-3.

[33] A. Das, R. Jurk, K.W. Stöckelhuber, and G. Heinrich, "Effect of Vulcanization Ingredients on the Intercalation-Exfoliation Process of Layered Silicate in an Acrylonitrile Butadiene Rubber Matrix," *Macromol. Mater. Eng.*, vol. 293, no. 6, pp. 479–490.2008, doi: 10.1002/mame.200700375.

[34] D. Ondrušová *et al.*, "Targeted modification of the composition of polymer systems for industrial applications," *Bull. Pol. Acad. Sci. Tech. Sci*., vol. 69, no. 2, p. e136721, 2021, doi: 10.24425/bpasts.2021.136721.

[35] Z. Li, F. Wen, M. Hussain, Y. Song, and Q. Zheng, "Scaling laws of Mullins effect in nitrile butadiene rubbernanocomposites," *Polymer*, vol. 193, 2020, doi: 10.1016/j.polymer.2020.122350.

[36] R. Pyrz and B. Bochenek, "Discrete-continuum transition at interfaces ofnanocomposites," *Bull. Pol. Acad. Sci. Tech. Sci*., vol. 55, no. 2, pp. 251–260, 2007.

[37] S. Wang and S.A. Chester, "Modeling thermal recovery of the Mullins effect," *Mech. Mater.*, vol. 126, pp. 88–98, 2018, doi: 10.1016/j.mechmat.2018.08.002.

[38] Z. Li, H. Xu, X. Xia, Y. Song, and Q. Zheng, "Energy dissipation accompanying Mullins effect of nitrile butadiene rubber/carbon black nanocomposites," *Polymer*, vol. 171, pp. 106–114, 2019, doi: 10.1016/j.polymer.2019.03.043.

[39] H. Chu, J. Lin, D. Lei, J. Qian, and R. Xiao, "A network evolution model for recovery of the Mullins effect in filled rubbers," *Int. J. Appl. Mech.*, vol. 12, no. 9, p. 2050108, 2020, doi: 10.1142/S1758825120501082.

[40] L. Yan, D.A. Dillard, R.L. West, L.D. Lower, and G.V. Gordon, "Mullins effect recovery of a nanoparticle-filled polymer," *J. Polym. Sci. B Polym. Phys.*, vol. 48, no. 21, pp. 2207–2214, 2010, doi: 10.1002/polb.22102.